

Computational Modeling of the Vacuum Arc Remelting (VAR) Process Used for the Production of Ingots of Titanium Alloys

Kanchan M. Kelkar¹, Suhas.V. Patankar¹, Alec Mitchell², Osamu Kanou³, Nobuo Fukada³, Kenji Suzuki³

¹Innovative Research, Inc., 3025 Harbor Lane North, Plymouth, MN 55447, USA

²Department of Metals and Minerals Engineering, University of British Columbia, Vancouver, BC V6T 1Z4, Canada

³Titanium Division, Titanium Technology Department, TOHO Titanium Ltd., Chigasaki, Japan

In the present study, a comprehensive computational model for the prediction of the performance of the VAR process is presented. The computational model analyzes electromagnetics, turbulent flow in the metal pool, magnetic stirring, heat transfer, macrosegregation, and inclusion behavior for the duration of the entire melting process and after shutdown of melting. The effect of the arc is considered by specifying heat flux and current density distributions on the ingot surface. The flow field is calculated by solving unsteady mass and momentum conservation equations in presence of magnetic stirring. The two-equation k- ϵ model is used for the prediction of nonuniform turbulent mixing in the metal pool. The temperature distribution and the size of the molten pool are determined by solving the energy conservation equation that accounts for phase change, contact resistance at the ingot-mold interface, and heat loss to the bottom surface of the mold. The control-volume computational method incorporates several enhancements for treating ingot growth and process physics. The model has been applied for the analysis of practical process for Ti-64 to illustrate its ability in the detailed prediction of the pool evolution, thermal history, alloy concentrations in the final ingot, and inclusion behavior.

Keywords: Computational Modeling, Vacuum Arc Remelting, VAR, Titanium Alloys, Macroseggregation, Inclusion Behavior

1 Introduction

The Vacuum Arc Remelting process (VAR) is a type of consumable electrode remelting processes used for producing ingots of superalloys and Titanium. **Figure 1** shows a schematic diagram of the VAR process that uses a stationary water-cooled mold. The VAR process involves complex interactions of the electromagnetic, flow, and heat transfer processes. Mathematical modeling constitutes a scientific and cost-effective approach for developing a fundamental understanding of the governing physical processes and for predicting the effects of various operating parameters on process performance.

A number of studies involving computational analysis of the VAR process are presented in the literature. An analytical model of the electromagnetic phenomena in ESR and VAR processes is presented by Patel¹. A detailed analysis of heat transfer to the mold for various remelting processes is presented by Yu². Analyses of the flow and heat transfer phenomena in the VAR process are presented by Bertram et al.³ and Hans⁴. The study by Hans⁴ also includes analysis of macrosegregation.

The present study describes a comprehensive computational model of the VAR process that considers the electromagnetics, flow, heat transfer, phase change, macrosegregation, and inclusion behavior occurring within the ingot for axisymmetric conditions. The model performs transient analysis of the growing ingot for the entire process with or without magnetic stirring. Relative to earlier studies, the model presented in this study is deemed to be more complete due to its ability to predict inclusion behavior and more efficient in the analysis of both macrosegregation and ingot growth.

2 Mathematical Formulation

2.1 Assumptions

Practical VAR processes for casting of cylindrical ingots involve process conditions that are nearly invariant in the angular direction. Therefore, the assumption of axisymmetry results in both an accurate and computationally efficient model. The analysis uses a frame of reference attached to the top surface of the ingot. Thus, the computational domain expands downwards with the growing ingot. The behavior of the arc is modeled using an overall energy balance to determine boundary conditions on the top surface of the ingot.

2.2 Electromagnetics

The electromagnetic behavior for DC power is determined by solving a Laplace equation for electric potential. A specified fraction of the arc current enters the top surface of the ingot. The treatment of the outflow of current into the mold through the circumferential and bottom surfaces of the ingot accounts for the electrical resistance created by the progressive loss of contact due to ingot shrinkage. The in-plane (x-r) variations of the current density, Lorentz force, and the self-induced magnetic field are derived from the distribution of the electric potential.

When magnetic stirring is present, the interaction of the radial current density with the imposed oscillating axial magnetic field gives rise to an oscillating Lorentz force in the angular direction.

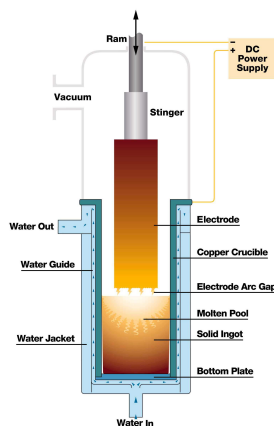


Figure 1. Schematic diagram of the Vacuum Arc Remelting (VAR) process (Courtesy ATI Allvac, 2003).

2.3 Fluid Motion

The in-plane (x-r) turbulent flow in the molten pool is governed by the unsteady mass and momentum conservation equations for the radial and axial velocities. This motion is driven by the combined action of Lorentz and buoyancy forces. When magnetic stirring is present, the resulting axisymmetric angular velocity field is determined by solving the corresponding momentum equation subject to the Lorentz force in the angular direction. Further, this rotational motion creates a centrifugal force that affects the radial velocity field. The effect of turbulent mixing is handled by using a turbulent viscosity.

The macro-level flow is assumed to be absent below the immobilization liquid fraction (λ_{immob}). This constitutes the boundary of the molten pool and the metal below this interface moves with the instantaneous casting velocity.

2.4 Energy Conservation

The unsteady energy conservation equation, with temperature as the primary unknown, is utilized for the calculation of the temperature distribution in the ingot. It involves a source term that arises due to the release of latent heat by the solidifying alloy. This term is calculated from the local liquid fraction λ which again is related to the temperature through an alloy-specific functional relationship.

The top surface of the ingot is subject to heating by the arc, radiative heat loss to the electrode, and inflow of metal with a prescribed superheat. Heat loss to the cooling water through the circumferential and the bottom surfaces of the ingot is analogous to the outflow of current into the mold. Thus, this calculation also accounts for the loss of contact due to the shrinkage of the ingot away from the mold.

2.5 Turbulent Mixing

It is important to note that the strength and the nonuniformity of mixing in the molten pool are dependent on the process conditions and are not known a priori. The present study used the two-equation k- ϵ model (Launder and Spalding⁵) for an automatic determination of the extent of turbulent mixing from the prevailing flow in the molten pool. It involves solution of transport equations for turbulent kinetic energy (k) and turbulent dissipation (ϵ) for calculating the variations of turbulent viscosity and turbulent conductivity. As a result, the computational model is very general and is valid over a wide range of ingot sizes and processing conditions.

2.6 Macrosegregation of Alloying Elements

Prediction of macrosegregation involves solution of convection-diffusion equations governing the concentrations of each of the alloying elements in the pool and the solid. The flow in the liquid pool penetrates only into the outer mushy region. The amount of solute rejected (absorbed) during this part of the solidification (up to a prescribed limiting liquid fraction λ^*) results in a source (sink) of that species in the liquid and a corresponding sink (source) in the solid. For each alloying element, this interface segregation flux is calculated from Scheil's equation with an equivalent segregation coefficient.

2.7 Behavior of Inclusions

An important objective of the VAR process is to remove any hard alpha and Titanium Nitride inclusions that may be present in the electrode. The motion and the dissolution of an inclusion are governed by Newton's law of motion involving the balance of inertia, drag, and buoyancy forces. The dissolution rate of an inclusion is assumed to be dependent on the temperature of the surrounding molten metal. Note that the time scale for the change in the pool size is large relative to the residence time of the inclusions. Hence, their motion is calculated at many time instants throughout the process based on the evolving flow and temperature fields within the molten pool.

3 Computational Solution

Computational solution of the governing equations is performed using the control volume technique of Patankar⁶. Several enhancements of the basic control volume method have been developed for the analysis of the VAR process. These include use of a Newton-Raphson linearization of the heat loss from ingot surfaces, an automatic determination of the time step, and a robust treatment of the temperature-dependent material properties.

The two significant enhancements include the treatment of ingot growth and the prediction of inclusion behavior. As the ingot grows, the bottom ingot-mold interface moves downward through the computational grid. Special consideration is given for constructing the discretization equations for the "base-plate" control volume because it expands in size within a time step due to ingot growth. Further, computational efficiency is achieved by limiting computational solution only to the control volumes that contain the ingot. Motion of inclusions is calculated by using a Lagrangian approach. It involves a time marching solution with an adaptive time step for the solution of the equations of motion and dissolution to determine the path of an inclusion and its evolving size.

4 Application of the Model

The computational method described above has been incorporated in the commercial software program COMPACT-VAR⁷. Its application for the analysis of a practical VAR process for Ti-64 is now discussed.

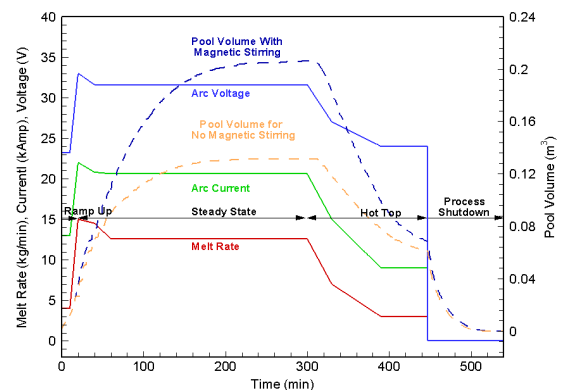


Figure 2. Process schedule and the predicted variation of the melt pool volume for the VAR process for Ti-64 alloy without and with stirring

Table 1. Physical properties of the Ti-64 alloy and operating conditions for the VAR process used in the application of the model.

| Geometry | |
|---|---|
| Electrode and Ingot Diameters | 660 mm, 760 mm |
| Initial and Final Ingot Lengths | 5 mm, 2.5 m |
| Alloy Properties (Ti-64) | |
| Density, Liquid | 3925 kg/m ³ |
| Viscosity, Liquid | 2.36x10 ⁻³ Pa-s |
| Solidus and Liquidus Temperatures | 1868 K, 1898 K |
| Latent Heat of Fusion | 7.6x10 ⁵ J/kg |
| Specific Heat, Liquid | 852 J/kg-K |
| Thermal Expansion Coeff., Liquid | 6.7x10 ⁻⁵ K ⁻¹ |
| Thermal Conductivity, Liquid | 29.7 W/m-K |
| Electric conductivity | 7.6x10 ⁵ (Ω-m) ⁻¹ |
| Magnetic permeability | 1.257x10 ⁻⁶ H/m |
| Segregation Coefficients for Al, V, Fe, O | 1.13, 0.95, 0.38, 1.33 |
| Electrode Concentrations of Al, V, Fe, O | 0.06125, 0.4, 0.004, 0.0016 |
| Operating Conditions | |
| Emissivity, Top Surface of Ingot | 0.5 |
| Electrode Sink Temperature | 2000 K |
| Emissivity, Ingot-Mold Heat Loss | 0.4 |
| Temperature of the Cooling Water | 313.15 K |
| Inlet Superheat | 100 K |
| Strength and Oscillation Period of the Axial Magnetic Field | 40 Gauss, 30 Seconds |

4.1 Physical Situation and Computational Details

Figure 2 shows the melt rate schedule for the VAR process for Ti-64 analyzed in this study. Note that analysis of the ingot behavior is continued even after melting has stopped. Table 1 gives the geometry, material properties, and operating conditions. Only representative values of temperature-dependent properties are listed.

A computational grid of 110(x)x40(r) control volumes is used in the analysis. Calculation for the entire process with no magnetic stirring requires about two hours on a

PC with a 3.2 GHz Intel processor. The analysis of the process with magnetic stirring requires about nine hours since a smaller time step is necessary to resolve the behavior of the stirring cycle.

4.2 Results and Discussion

The computational model predicts the electromagnetic, flow, temperature, and alloy concentrations fields, and inclusion motion in the ingot during the entire process. Important aspects of the results are now discussed with reference to Figures 2 to 6.

Figure 3 shows the variation of the electric current densities and the self-induced magnetic field in the growing ingot in the absence of magnetic stirring. Initially, the current entering the ingot flows out into the mold through both the circumferential and the bottom surfaces. When the ingot becomes long, very little current flows out from the bottom face. The current density interacts with the self-induced magnetic field to produce in-plane (x-r) Lorentz force field that is directed radially inwards and axially downwards.

Figure 4 shows the evolving flow and temperature fields in the ingot without and with magnetic stirring. When magnetic stirring is present, the stirring force produces an oscillating angular velocity field. The resulting strong centrifugal forces increase the in-plane

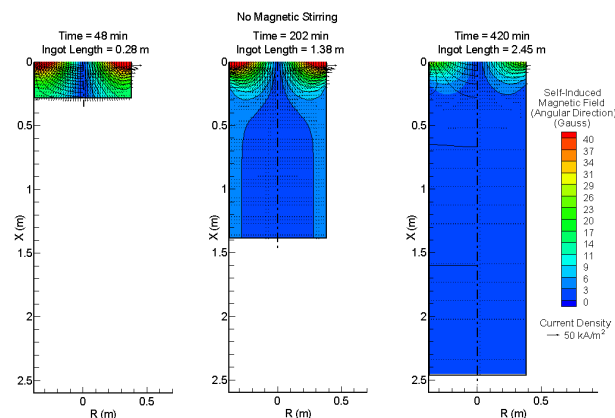


Figure 3. Field variations of the current density and self-induced magnetic field in the ingot during the VAR process for Ti-64 alloy without magnetic stirring.

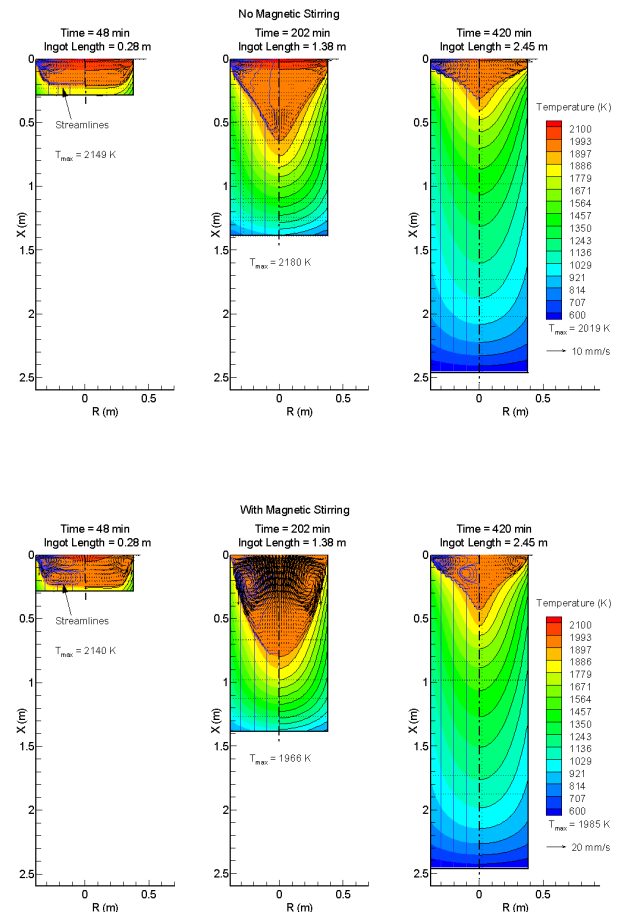


Figure 4. Flow and temperature fields in the ingot during the VAR process for Ti-64 alloy without and with magnetic stirring.

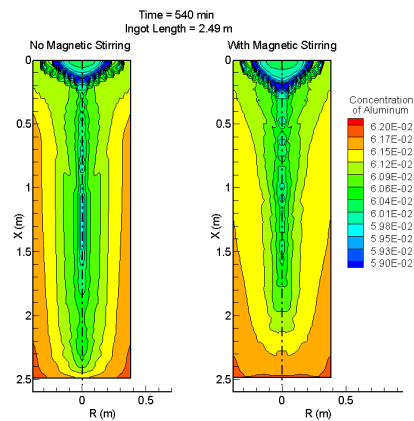


Figure 5. Variation of Aluminum concentration in the ingot after shutdown of the VAR process for Ti-64 alloy without and with magnetic stirring

motion. This increased mixing reduces thermal gradients within the pool (lower maximum temperature) and makes the pool more parabolic in shape. The increase in pool volume in presence of stirring is also seen in **Fig. 2**.

The capability of the model for predicting macrosegregation of alloying elements is illustrated in **Fig. 5**. It shows the variation of Aluminum concentration in the ingot at a time instant after melting has stopped and the ingot has cooled sufficiently so that there is no macro-scale motion. Note that during the solidification process, Aluminum is preferentially absorbed by the solid (segregation coefficient greater than unity). As the ingot grows, the average concentration of Aluminum in the liquid pool decreases. Therefore, the concentration of Aluminum in the upper portion of the ingot (formed later in the process) is lower than that in the lower portion of the ingot (formed earlier in the process). Further, the concentration of Aluminum is low in the center portion of the pool. This is because the flow at the bottom of the pool is weak and it does not sufficiently replenish the Aluminum absorbed by the newly formed solid in the center region. The increased mixing present when magnetic stirring is used is seen to significantly reduce macrosegregation in the radial direction. The model also predicts macrosegregation of Vanadium, Iron, and Oxygen in the solidified ingot. Due to space constraints, the corresponding concentration plots are not included.

The trajectories of light, neutrally buoyant, and heavy inclusions of different sizes (0.1 mm to 5 mm diameter) are shown in **Fig. 6** at a time instant at which the pool volume has nearly attained its maximum value. All inclusions are introduced at uniformly spaced locations on the top surface of the ingot. Inclusions that are either small in size or are neutrally buoyant move with the molten metal. Most of the small inclusions are found to dissolve. The motion of large inclusions is strongly influenced by their density relative to the liquid metal. Large heavy inclusions go quickly to the bottom of the pool and get trapped in the mushy region while light inclusions float to the top of the pool, move radially outwards, and tend to spend a significantly more time in the pool. Finally, in the presence of stirring, inclusions

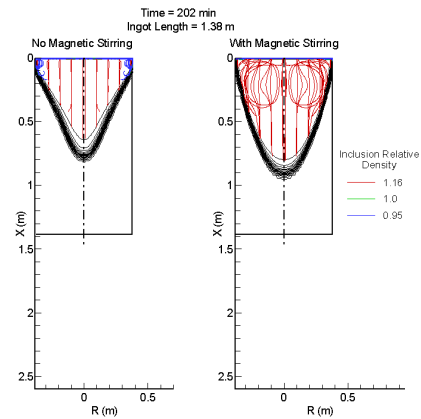


Figure 6. Trajectories of inclusions of different sizes and densities at a representative time instant during the VAR process for Ti-64 alloy without and with magnetic stirring.

spend a longer time within the pool due to stronger in-plane velocities as well as motion in the angular direction. After the calculation of the behavior of inclusions of various sizes and densities is completed for a specific instant during the process, the fraction of each type of inclusion that survives is calculated. Further, the distribution of the ending locations of the surviving inclusions is also determined.

5 Summary and Conclusions

The present study describes a comprehensive, robust, and efficient computational model for transient analysis of electromagnetic, flow, heat transfer and macrosegregation phenomena, and inclusion behavior in practical VAR processes. The model has been applied for the analysis of VAR process of Ti-64 alloy. The results provide insights into the physical phenomena that govern the process behavior. Further, quantitative information about the process performance obtained from the model is of significant utility in optimizing process operation so as to produce ingots with the desired composition and microstructure.

REFERENCES

1. A.D. Patel, *Proc. of Liquid Metal Processing and Casting*, ed. P. D. Lee, A. Mitchell, J. Bellot, and A. Jardy, (AVS), (2003), pp. 205-214.
2. Yu Kuang-O, *Proc. Vacuum Metallurgy Conference*, ed. G.K Bhat and L.W. Lherbier, (AVS), (1984) pp. 83-92.
3. L.A. Bertram, C.B. Adaszczik, D.G. Evans, R.S. Minisandram, P.A. Sackinger., D.D. Wegman., R.L. Williamson, *Proc. of Liquid Metal Processing and Casting*, ed. A. Mitchell and P. Aubertin, (AVS), (1997), pp. 110-132.
4. S. Hans., Ph.D. Thesis (in French), Ecole Des Mines, (1995), Nancy, France.
5. B.E. Launder and D.B. Spalding, *Comp. Meth. in Appl. Mech. and Eng.*, **3** (1974), pp. 269-281, 1974.
6. S.V. Patankar, *Numerical Heat Transfer and Fluid Flow*, (1980), Hemisphere Publishing Corporation, Washington
7. COMPACT-VAR Reference Manual, (2006), Innovative Research, Inc., 3025 Harbor Lane N., Suite 300, Plymouth, MN 55447, www.inres.com.